



**HAL**  
open science

## Seasonal and inter-annual variability in abundance of the main tropical tunas in the EEZ of Côte d'Ivoire (2000-2019)

Sosthène Akia, M. Amande, P. Pascual, Daniel Gaertner

► **To cite this version:**

Sosthène Akia, M. Amande, P. Pascual, Daniel Gaertner. Seasonal and inter-annual variability in abundance of the main tropical tunas in the EEZ of Côte d'Ivoire (2000-2019). *Fisheries Research*, 2021, 243, pp.106053. 10.1016/j.fishres.2021.106053 . hal-03451165

**HAL Id: hal-03451165**

<https://hal.umontpellier.fr/hal-03451165v1>

Submitted on 2 Aug 2023

**HAL** is a multi-disciplinary open access archive for the deposit and dissemination of scientific research documents, whether they are published or not. The documents may come from teaching and research institutions in France or abroad, or from public or private research centers.

L'archive ouverte pluridisciplinaire **HAL**, est destinée au dépôt et à la diffusion de documents scientifiques de niveau recherche, publiés ou non, émanant des établissements d'enseignement et de recherche français ou étrangers, des laboratoires publics ou privés.



Distributed under a Creative Commons Attribution - NonCommercial 4.0 International License

# 1 Seasonal and inter-annual variability in abundance of the main 2 tropical tunas in the EEZ of Côte d'Ivoire (2000-2019)

3 Akia S<sup>1,2,3\*</sup>, Amandé M<sup>2</sup>, Pascual P<sup>4</sup>, and Gaertner D<sup>1,3</sup>.

## 4 Abstract

5 The seasonal and inter-annual variability in abundance of the main “local tropical tuna  
6 resources” in the EEZ of Côte d'Ivoire was analysed with catch and effort data from French  
7 and Spanish purse seiners over the period 2000-2019. A seasonal spatio-temporal model  
8 developed by Thorson et al. (2020a) was used to estimate abundance indices for the main  
9 tropical tunas by commercial category (<10kg and ≥10kg, which correspond roughly to  
10 maturity stage: immature and mature respectively), and fishing mode (free school sets and  
11 FAD sets). Furthermore, we decomposed the abundance time series into intrinsic mode  
12 functions using the CEEMDAN algorithm. The decomposition procedure made it possible to  
13 filter out the noise in the signal and extract the seasonal and inter-annual components of the  
14 abundance indices. A generalized additive model (GAM) was applied to the abundance  
15 indices to reveal the influences of environmental factors on species abundance and spatio-  
16 temporal distribution. Biological interpretations of the seasonal and inter-annual variability in  
17 tropical tuna abundance were made and the possible effects of environmental variables on this  
18 abundance discussed. Our results suggest that there are two main fishing seasons in the EEZ  
19 of Côte d'Ivoire. It was also found that mature yellowfin tunas are abundant between the first  
20 and second quarter of the year while the best season for skipjack occurs between the third and  
21 fourth quarter. In addition, we observed a considerable change over time in the seasonal and  
22 inter-annual variability of tropical tunas in this area.

23 **Keywords:** abundance indices, seasonal and inter-annual variation, spatio-temporal vector  
24 autoregressive model (VAST), tropical tuna.

## 25 Highlights

- 26 • Assessment of the tuna resources in the Exclusive Economic Zone (EEZ) of Côte  
27 d'Ivoire by estimating abundance indices with a seasonal spatio-temporal model.
- 28 • Evidence of two marked seasons of abundance in the study area: mature yellowfin  
29 from February to June and skipjack from August to December.
- 30 • Differences in behaviour (month of peak abundance, sensitivity to environmental  
31 variables) of tuna caught on Fish Aggregating Devices (FAD) vs tuna caught on Free-  
32 Swimming Schools (FSC).
- 33 • Similarity between the dynamics of some abundance indices and some environmental  
34 variables.

35 <sup>1</sup> MARBEC, Univ Montpellier, CNRS, Ifremer, IRD, Sète, France

<sup>2</sup> Centre de Recherches Océanologiques (CRO), Abidjan, Côte d'Ivoire

<sup>3</sup> Institut de Recherche pour le Développement (IRD), UMR MARBEC, Av. Jean Monnet, CS 30171, Sète Cedex 34203, France

<sup>4</sup> Instituto Español de Oceanografía. Centro Oceanográfico de Canarias. Apdo. de Correos 1373. 38080. Santa Cruz de Tenerife. Islas Canarias (ESPAÑA).

\*Corresponding author at: UMR MARBEC, Avenue Jean Monnet CS 30171, Sète, CEDEX 34203, France.

E-mail address: [sosthene.akia@ird.fr](mailto:sosthene.akia@ird.fr) (S. AKIA)

## 36 1. Introduction

37 Fishing is of paramount importance in Côte d'Ivoire, as it is one of the main sources of animal  
38 protein for the country's poorest households due to its relatively affordable price compared to  
39 meat. Socio-economically, the tuna industry plays an important role in employment in Côte  
40 d'Ivoire (landing activities, canneries) and exports there. A trade and utilization chain for the  
41 tuna bycatch, called "faux poissons", retained on-board by purse seiners and landed in  
42 Abidjan (Côte d'Ivoire) has been developed since the early 1990s. Romagny et al. (2000)  
43 showed that this sector was of great socioeconomic importance for its actors from landing to  
44 consumption. A recent study has shown that in addition to the great social and economic  
45 importance of this sector for the local population, it contributes substantially towards food  
46 security for the Ivorian people (Monin et al., 2017). Côte d'Ivoire furthermore benefits from  
47 the incomes generated by fisheries agreements concluded with long-distance foreign vessels.

48 Given the essential role of fisheries, and mainly tuna fisheries, coastal countries have  
49 established fisheries departments to better manage the exploitation of tuna resources in their  
50 EEZ. Due to their highly migratory nature, the management of tuna stocks is carried out at a  
51 large regional scale by Regional Fisheries Management Organizations (RFMOs). Despite the  
52 need to assess the status of tuna resources at the stock level, little information is produced to  
53 know the state of the local resources, thus the coastal countries cannot optimize the  
54 management of their EEZ. In Côte d'Ivoire, there are two main types of tuna fisheries:  
55 industrial and artisanal. Industrial fisheries are dominated by EU purse seiners, with Spain and  
56 France predominant (Failler et al., 2014). Fisheries data for the EU industrial fleet are very  
57 well collected and monitored, and remain the best sources of information on the sector. The  
58 tuna resources of Côte d'Ivoire are mainly exploited by this fleet within the framework of a  
59 fishing agreement between Côte d'Ivoire and the European Union (Failler et al., 2014). The  
60 production of artisanal tuna fishery remains significant, but the data collected on this segment  
61 remain insufficient for a complete analysis of the sector. To date, local abundance of tuna in  
62 the EEZ of Côte d'Ivoire has not been specifically assessed (Cofrepeche, Poseidon, 2012;  
63 Failler et al., 2014). However, the downward trend in the reference tonnage of the EU/CIV  
64 fisheries agreements (supplementary material S1: Table 1:S1) and the global and local effects  
65 of climate change highlight the urgent need for Côte d'Ivoire to study seasonal and inter-  
66 annual variation in the tuna resources temporarily found in its EEZ.

67 Given the lack of direct estimates from scientific surveys, commercial catch per unit of  
68 effort (CPUE) is used to derive relative abundance of tuna resources which play an important  
69 role in stock assessment and management (Ricker, 1940; Maunder and Langley, 2004;  
70 Maunder and Punt, 2004). Nominal CPUEs derived from commercial fisheries are greatly  
71 influenced by spatial, temporal, and environmental factors, among others, and need to be  
72 standardized (Fonteneau et al., 1999; Maunder and Punt, 2004). Several methods have been  
73 applied to standardize CPUE including GLMs and GAMs (Campbell, 2004; Katara et al.,  
74 2018); machine learning and data mining techniques (Albeare, 2009; Yang et al., 2015), and  
75 spatio-temporal models (Maunder et al., 2020; Thorson et al., 2020b). We use the recent  
76 version of the VAST spatio-temporal model developed by Thorson et al. (2020a). This model  
77 includes annual, seasonal and spatial variations in density and allows us to capture two  
78 important key issues: (i) the standardization of data that are spatially unbalanced over several  
79 seasons and (ii) the identification of inter-annual changes in the seasonal chronology of  
80 population. The three most important tropical tuna species - skipjack tuna (*Katsuwonus*  
81 *pelamis*, SKJ), yellowfin tuna (*Thunnus albacares*, YFT), and bigeye tuna (*Thunnus obesus*,  
82 BET) - were divided into eight class categories taking into account the species, the maturity  
83 stage (immature and mature), and the two main fishing modes in the purse seine fishery (free  
84 school sets and floating object sets: hereafter referred to as FSC and FOB, respectively [note  
85 that FOB can be natural logs but in the large majority of cases are drifting fish aggregating

86 devices known as dFADs]. The categorization of species by school type is legitimate in the  
87 sense that the fishing techniques differ. Fishing on dFADs can be analogous to harvesting and  
88 collecting, and fishing on free schools to searching and hunting. dFADs increase the  
89 catchability of tuna, as compared to sets on free schools by helping fishers locate fish  
90 (reducing search time) and allowing a high percentage of successful sets (Moreno et al.,  
91 2007). Free schools are dominated by large yellowfin whereas dFADs schools are mainly  
92 composed of skipjack and juveniles of the two others species. This distinction will enable  
93 evaluation of this aspect in the study area. Several studies have highlighted the major effects  
94 of climatic cycles on the distribution and availability of tuna resources in a local area (Maury  
95 et al., 2001; Lehodey et al., 2006; Ménard et al., 2007; Marsac, 2017). The variability of  
96 climatic conditions can be a non-negligible indicator of the variability in tuna abundance and  
97 spatial distribution and consequently justify the analysis of the relationship between  
98 environmental variables and tuna abundance indices. The following environmental variables  
99 have been selected for this study: sea surface temperature (SST), dissolved oxygen at a depth  
100 of 100 meters (DO2\_100), chlorophyll concentration (CHL), sea surface salinity (SSS), mixed  
101 layer thickness (MLD), sea surface height (SSH) and SST-based coastal upwelling index  
102 (CUI\_sst). Indeed, some studies showed that upwelling indices are important in explaining the  
103 fluctuations of tuna and tuna-like species abundance (Cury and Roy, 1987; Roudaut, 1999).

104 To analyse the seasonal and inter-annual variation in the European purse seiners CPUEs in  
105 the Ivorian EEZ, we first estimated the abundance indices using a Thorson et al. (2020a)  
106 seasonal spatio-temporal model. Thereafter, we used a method adapted to analyse non-linear  
107 and non-stationary signals (i.e., the CEEMDAN algorithm), with the aim to decompose the  
108 CPUE series into a finite and exhaustive number of components, called intrinsic mode  
109 functions (IMFs). Finally, we explored the relationships between the estimated abundance  
110 indices and the environmental variables using GAMs.

## 111 **2. Materials and methods**

### 112 *2.1 Study area*

113 The study area extends between latitudes 1°N and 6°N and longitudes 2°W and 8°W (Fig. 1).  
114 This is the smallest area that includes the 1° square that pass through the Ivorian EEZ. The  
115 area was selected to facilitate future comparisons with data collected by 1° square degrees and  
116 to avoid boundary effects. This area is characterized by a seasonal surface temperature signal  
117 due to the presence of two cool seasons, each associated with the coastal upwelling (Morlière,  
118 1970). The main cold season takes place in winter between July and September. Winter  
119 cooling is then intensified on the coast by upwelling that brings nutrient-rich water to the  
120 surface. A second cooling occurs along the coast in January-February; this second cold season  
121 is low-amplitude and short-lived (between one and two months; Cury and Roy, 1987)

### 122 *2.2 Catch and effort data*

123 Catch and effort data for EU purse seiners operating in the EEZ of Côte d'Ivoire from 2000 to  
124 2019 were compiled and managed by the Tuna Observatory (Ob7) of the French National  
125 Research Institute for Sustainable Development (IRD, UMR MARBEC), and the Spanish  
126 Institute of Oceanography (IEO) for the French and the Spanish fleets respectively. The raw  
127 logbook data produced by the skippers were corrected by the T3 methodology regarding total  
128 catch per set (to account for the difference between reported catch at sea and landed catch)  
129 and species composition (based on port size sampling), see Pallarés and Hallier (1997) and  
130 Duparc et al. (2020), to generate the level 1 logbook database used in this paper. The  
131 commercial size category was used as a discriminant factor at the maturity stage of bigeye and  
132 yellowfin tuna. Commercial categories 2 and 3 (tuna  $\geq 10$  kg) are classified as mature and  
133 category 1 (tuna  $< 10$  kg) is classified as immature (except for skipjack which belongs to this

134 category and was not divided by maturity stage). We know from the literature<sup>5</sup> that 50% size  
135 at maturity is reached around 100cm fork length (that is to say around 20kg) for yellowfin and  
136 bigeye. However, for the sake of simplicity we used the conventional “size” commercial  
137 categories reported in purse seiners logbooks by European skippers (category 1: <10kg;  
138 category 2: 10 to 30kg; category 3: >30kg). All sets per boat and per day were combined and  
139 assigned to the centroids of these activities. The total number of sets per day per boat has been  
140 filtered and days with unrealistic data (over 5 sets per day per boat) deleted. Given that free  
141 schools are detected at random at the surface of the sea, the unit of effort associated with this  
142 fishing mode was expressed as the searching time (i.e., the time spent on the fishing ground  
143 less the duration of all setting operations). In contrast, many dFADs are not encountered  
144 randomly, specifically when they are equipped with a GPS buoy and continuously tracked  
145 remotely by the purse seiner. In such a case we used the number of dFADs sets as a  
146 measurement of the fishing effort. The data were then divided into eight categories according  
147 to the species, the maturity stage and the fishing mode. Only catch and effort data from sets  
148 conducted out in the study area were selected in this study.

### 149 *2.3 Environmental data*

150 Six candidate environmental variables were extracted from the EU's Copernicus Marine  
151 Environment Monitoring Service (CMEMS) (<https://marine.copernicus.eu/>) at a monthly  
152 mean resolution (Table 1): sea surface temperature (SST), sea surface height (SSH),  
153 chlorophyll concentration (CHL), salinity (SSS), mixed-layer thickness (MLD), and dissolved  
154 oxygen at a depth of 100 meters (DO2\_100). The spatial resolution of the model grid for SSS,  
155 SSH, SST, and MLD is 1/12° (0.083° x 0.083°, about 8 km), while the spatial resolution for  
156 CHL, DO2\_100 is 1/4° (0.25° x 0.25°, about 24 km).

### 157 *2.4 Coastal upwelling index (CUI\_SST)*

158 A seventh environmental variable, the monthly SST-based coastal upwelling index  
159 (CUI\_SST) was calculated for the Ivorian EEZ. The SST-based coastal upwelling indices are  
160 obtained by taking the thermal difference ( $\Delta T$ ) between the coast and the offshore SST at the  
161 same latitude. In practice, CUI\_SST has been defined as the thermal difference between cold  
162 coastal waters and warmer offshore waters at the same latitude (Benazzouz et al., 2014). The  
163 general formulation is as follows:

$$164 \quad CUI_{SST}(\text{lat, time}) = SST_{\text{offshore}}(\text{lat, time}) - SST_{\text{coastal}}(\text{lat, time}) \quad (1)$$

165 The general calculation formula is very simple, but the challenge is to study the best way to  
166 define the coastal and offshore zones and to correctly extract the two thermal references to be  
167 used for the calculation. The resulting SST-based coastal upwelling index is characterized by  
168 a seasonal signal with peaks in the first and third quarter of the year (Fig. 2).

## 169 *2.5 Methods*

### 170 *2.5.1 The seasonal spatio-temporal model*

171 We applied a vector-autoregressive spatio-temporal delta-generalized linear mixed model to  
172 the catch and effort data, using the R package VAST (Thorson, 2019). Recently, VAST has  
173 been expanded to account for seasonal and inter-annual variability (Thorson et al., 2020a).  
174 This allows an understanding how species distribution and abundance varies within a year by  
175 month or season, and also within a month or season across years. It offers reasonable  
176 performance even when data are not fully available for one or more combinations of years and

---

<sup>5</sup> See ICCAT manual, chapter 2 at <https://www.iccat.int/en/iccatmanual.html>

177 seasons, which is common in commercial catch data. In order to work at a finer scale  
 178 temporal resolution (monthly, bi-monthly, quarterly...), the estimates in year-season  $t$  are  
 179 shrunk towards predicting density in adjacent year-seasons ( $t-1$  and  $t+1$ ), as well as towards  
 180 estimating density in other seasons in a given year and density in other years for a given  
 181 season. This specification implies that the model includes a “main effect” for a season and  
 182 year, as well as an autocorrelated “interaction” of season and year. We present below a brief  
 183 summary of the principal parameters and philosophy of the model but readers are encouraged  
 184 to refer to supplementary materials S2 for more technical details.

185 The VAST model is being implemented using the Poisson-link delta model as  
 186 recommended by Thorson (2018). The Poisson-link delta model includes the probability  $p_i$   
 187 that sample  $i$  encounters a given species [i.e.  $\Pr(B > 0)$ ], and also the expected measurement  
 188  $r_i$  given that species is encountered,  $\Pr(B | B > 0)$ :  
 189

$$190 \Pr(B = b_i) = \begin{cases} 1 - p_i & \text{if } B = 0 \\ p_i \times g\{B | r_i, \sigma_m^2\} & \text{if } B > 0 \end{cases} \quad (2)$$

191 where we specify a lognormal distribution for positive catches. This Poisson-link delta model  
 192 predicts encounter probability  $p_i$  and positive catch rate  $r_i$  by modeling two log-linked linear  
 193 predictors,  $\log(n_i)$  and  $\log(w_i)$  for each sample  $i$ ;  $n_i$  and  $w_i$  are then transformed to yield  $p_i$   
 194 and  $r_i$  :

$$196 p_i = 1 - \exp(-a_i \times n_i), r_i = \frac{a_i \times n_i}{p_i} \times w_i, \quad (3)$$

197 where  $a_i$  is the area-swept offset for sample  $i$ . This model structure is designed so that  
 198 expected density  $d_i$  is the product of encounter probability and positive catch rate and also the  
 199 product of transformed linear predictors (i.e.  $d_i = p_i * r_i = n_i * w_i$ ). These predictors can be  
 200 interpreted as numbers-density  $n_i$  (with units numbers per area) and average weights  $w_i$  (with  
 201 units biomass per number).  $n_i$  always enters via the product  $a_i * n_i$  such that  $n_i$  is expressed  
 202 as density. We consider effort as a catchability factor in the model. The Poisson-link delta  
 203 model is useful relative to other delta models because both linear predictors use a log-link  
 204 function so that all effects are additive in their impact on the predicted log-density.  
 205 Specifically, we specify that:  
 206

$$208 \log(n_i) = \underbrace{\beta_n^*(t_i)}_{\text{Year-season intercept}} + \underbrace{\omega_n^*(s_i)}_{\text{Spatial main effect}} + \underbrace{\xi_{nu}^*(s_i, u_i)}_{\text{Season spatial effect}} + \underbrace{\xi_{ny}^*(s_i, y_i)}_{\text{Year spatial effect}} + \underbrace{\varepsilon_{nu}^*(s_i, t_i)}_{\text{Year-season spatial effect}} + \underbrace{\zeta_n^*(i)}_{\text{Catchability covariates}} \quad (4)$$

$$212 \log(w_i) = \underbrace{\beta_w^*(t_i)}_{\text{Year-season intercept}} + \underbrace{\omega_w^*(s_i)}_{\text{Spatial main effect}} + \underbrace{\xi_{wu}^*(s_i, u_i)}_{\text{Season spatial effect}} + \underbrace{\xi_{wy}^*(s_i, y_i)}_{\text{Year spatial effect}} + \underbrace{\varepsilon_{wu}^*(s_i, t_i)}_{\text{Year-season spatial effect}} + \underbrace{\zeta_w^*(i)}_{\text{Catchability covariates}} \quad (5)$$

214 The French purse seiners were targeting mainly free schools while the Spanish purse  
 215 seiners were targeting drifting FADs. This difference in fishing strategy is less pronounced in  
 216 the recent years as the use of dFADs-fishing increased in both fleets. There is likely also a  
 217 vessel size category component in the choice of the fishing strategy. Both covariates (flag and  
 218 vessel size category [carrying capacity]) have been introduced in the analysis as catchability  
 219 covariates as suggested by Thorson (2019).

220 Key model parameters for abundance indices are density predicted, area-weighted density  
 221 sum, and abundance-weighted mean density. The model estimates the density prediction per  
 222 year at each fine spatial resolution:

$$\begin{aligned}
 d(s, t) &= n(s, t) \times w(s, t) \\
 &= \exp\{\beta_n^*(t) + \omega_n^*(s) + \xi_{nu}^*(s, u) + \xi_{ny}^*(s, y) + \varepsilon_n^*(s, t) + \zeta_n^*\} \\
 &\quad \times \exp\{\beta_w^*(t) + \omega_w^*(s) + \xi_{wu}^*(s, u) + \xi_{wy}^*(s, y) + \varepsilon_w^*(s, t) + \zeta_w^*\}
 \end{aligned} \tag{6}$$

224  
 225 We use density to calculate the total abundance for the entire domain as the area-weighted  
 226 sum of density  $d(s, t)$  predicted at a fine spatial resolution:

$$I(t) = \sum_{s=1}^{n_s} a(s)d(s, t) \tag{7}$$

229 where  $n_s$  is the number of fine-scale predictions and  $a_s$  is the spatial area associated with  
 231 each prediction. See the supplementary material S2 for more details on the model, its  
 232 implementation and results.

### 233 2.5.2 Statistical analyses

234 We decomposed the abundance indices into intrinsic mode functions to extract their seasonal  
 235 and inter-annual components using the Complete Ensemble Empirical Mode Decomposition  
 236 with adaptive noise (CEEMDAN) algorithm. The CEEMDAN algorithm belongs to the broad  
 237 family of Empirical Mode Decomposition (EMD) algorithms (Huang et al., 1998). Torres et  
 238 al. (2011) introduced this algorithm as a variation of the EEMD algorithm (Wu and Huang,  
 239 2009) that allows exact reconstruction of the original signal and better spectral separation of  
 240 intrinsic mode functions. We used the package "Rlibeemd" (Luukko et al., 2016) to  
 241 decompose the eight abundance indices using the CEEMDAN algorithm. See the  
 242 supplementary material S1 for more details on the CEEMDAN algorithm application.

243 The seasonal and inter-annual components of the abundance indices estimated in this  
 244 paper are extracted from the CEEMDAN intrinsic mode functions (IMFs). The residual  
 245 component represents the long-term component (inter-annual component), and the IMFs with  
 246 annual frequency represent the seasonal (intra-annual) component. Three types of time series  
 247 in the different IMFs can be observed: (i) some sub-annual (periodic) time series showing at  
 248 least two local minimum and two local maximum by year (ii) the annual (periodic) time series  
 249 that had no more than three local peaks (maximum + minimum) and (iii) some supra-annual  
 250 (periodic) time series. In situations when there was more than one annual frequency  
 251 component, we considered the average between them to construct the seasonal component.  
 252 The seasonal component was used for two purposes in this study. First, we calculated the  
 253 average abundance per season (month or two months in the case of immature yellowfin tuna  
 254 caught on dFADs) over the entire study period. This allowed us to have the average seasonal  
 255 factors. Then, we examined the dynamics of seasonality over the entire study period. The  
 256 packages seasonal (Sax and Eddelbuettel, 2018) and forecast (Hyndman and Khandakar,  
 257 2008) were used for plotting the inter-annual variation of the seasonalities of each abundance  
 258 index.

259 A Principal Component Analysis (PCA) was used to understand the common variability  
 260 of the environmental variables used and to characterize environmental conditions of tropical  
 261 tunas in the EEZ of Côte d'Ivoire.

262 GAMs (Hastie and Tibshirani, 1987) were used to study the links between the abundance  
 263 indices by category and the environmental factors because they make it possible to take into  
 264 account the non-linearity of such relationships (Maury et al., 2001). GAMs allowed the  
 265 quantification of the percentage of deviance that can be explained by habitat, and to determine

266 the relative contribution of the environmental variables. All statistical analyses were  
267 conducted with R 4.2. (R Core Team, 2019). The packages FactoMineR 1.34 (Husson, 2008)  
268 and mgcv 1.8–31 (Wood, 2017) were used for PCAs and for GAMs, respectively. The entire  
269 data processing and analysis procedure is summarized in Fig.3.

### 270 **3. Results**

271 Supplementary material S2 presents the estimated abundance indices and the decomposition  
272 of each abundance index into intrinsic mode functions using the CEEMDAN algorithm. All  
273 these results were analysed to obtain the factors related to the seasonal and inter-annual  
274 variation in the abundance of tropical tunas in the area of the EEZ of Côte d'Ivoire.

#### 275 *3.1 Seasonality of abundance indices*

276 Mature yellowfin tuna captured on FSC and skipjack tuna captured on dFADs in the Ivorian  
277 EEZ are the categories showing the most obvious seasonality (Fig. 4). The seasonality of the  
278 tuna fisheries in the EEZ of Côte d'Ivoire is largely due to these two species. Two main tuna-  
279 abundance seasons can be identified. The first, characterized by an abundance of mature  
280 yellowfin tuna, takes place between March and July, and the second, characterized by an  
281 abundance of skipjack tuna, takes place between August and December (Fig. 4; Table 2).  
282 Some shrinkage of the seasonality factor is evident for SKJ on FSC, with amplitude ranging  
283 from 23 at the start of the study period to almost 5 over the last years (Fig. 5). The seasonality  
284 of the other abundance indices is almost constant throughout the study period (Fig. 5; Fig. 6).

#### 285 *3.2 Inter-annual variations of abundance indices*

286 For sets on dFADs, there is a general downward trend in abundance indices for the majority  
287 of the categories (Fig. 7). The abundance indices for mature bigeye tuna show a downward  
288 trend from 2000 to 2009 and an upward trend since 2009.

289 For sets on FSC, there is an overall downward trend in the abundance indices for  
290 immature yellowfin tuna and skipjack tuna from 2000 to 2016/2017 and an upward trend from  
291 2016/2017 onwards (Fig. 7). Mature yellowfin tuna increase over the study period. Mature  
292 bigeye tuna tend to increase from 2000 to 2006, then decrease to a local minimum in 2014  
293 and increase from 2015 to 2019. Mature yellowfin tuna is the predominant category in the  
294 FSC species composition.

#### 295 *3.3 Environmental variability in the study area (PCA results)*

296 The criterion of Kaiser (1960) enables the selection of the first three axes that represent 82.9%  
297 of the total variability contained in the environmental variables. PCA showed correspondence  
298 between chlorophyll concentration (CHL), coastal upwelling index (CUI\_sst) and sea surface  
299 salinity (SSS), which were strongly correlated to the positive semi axis of the first principal  
300 component, and opposed to sea surface temperature (SST) and sea surface height (SSH)  
301 (Table 3; Fig. 8). The first principal component (Dim 1), explained 53.6% of the global  
302 variability of the data, highlights the great difference in environmental conditions between the  
303 primary cold season characterized by the upwelling phenomena and the primary warm season.  
304 From the projection of the months over the first two axes, it can be seen that July, August, and  
305 September are on the positive semi axis of the first principal component (Dim1), and April  
306 and May are on the negative semi axis of that first component (Supplementary material S1:  
307 Fig. 9:S1).

308 The second component of this PCA explained 16.2% of the global variability of the data.  
309 It was strongly correlated to the mixed-layer thickness (MLD) on the positive semi-axes  
310 (Table 3). This second component (Dim 2) was interpreted as a mixed layer depth gradient.  
311 From the projection of the months over the first two axes, it can be seen that June is on the



312 positive semi axis of the second principal component (Dim2) (Supplementary material S1:  
313 Fig. 9:S1).

314 The third component of this PCA explained 12.3% of the global variability of the data  
315 (Fig. 8). It was strongly correlated to the dissolved oxygen at a depth of 100 meters  
316 (DO2\_100) on the positive semi-axis (Table 3). This third component (Dim 3) was interpreted  
317 as a dissolved oxygen gradient which is a sub-surface variable.

### 318 *3.4 Results of GAM models*

319 All environmental variables were significant in terms of explaining the variability of skipjack  
320 abundance indices. There are however some differences between the abundance on FSC that  
321 is better explained by dissolved oxygen at a depth of 100 meters (DO2\_100), salinity, sea  
322 surface temperature (SST), chlorophyll concentration (CHL) and mixed-layer thickness  
323 (MLD), while abundance indices on dFADs are better explained by dissolved oxygen at 100  
324 meter depth (DO2\_100) (Table 4).

325 Abundance index for adult yellowfin tunas on dFADs is explained by sea surface height  
326 (SSH), sea surface temperature (SST), chlorophyll concentration (CHL) and coastal upwelling  
327 index (CUI\_sst) while abundance on FSC is linked to sea surface temperature (SST) only,  
328 with a higher proportion of the deviance explained for dFADs (Table 4).

329 Only the dissolved oxygen at a depth of 100 meters (DO2\_100) better explains abundance  
330 indices for juvenile yellowfin tunas (on dFADs and on FSC). It must be stressed that the  
331 deviance explained by environmental factors on the abundance on dFADs is higher than those  
332 FSC (Table 4).

333 For mature bigeye tunas, abundance indices on dFADs are better explained by sea surface  
334 temperature (SST) and chlorophyll concentration (CHL) while for FSC sea surface  
335 temperature (SST) and mixed-layer thickness (MLD) are the two environmental factors that  
336 most impact on the abundance.

## 337 **4. Discussion**

338 The need for coastal countries to evaluate their local resources is gaining importance.  
339 Andriamahefazafy (2020) highlighted that the inability for coastal countries to evaluate their  
340 tuna resources was frustrating for their governments. This highlights their willingness and  
341 need to gain an idea of the variability of the abundance of tuna transiting their EEZs as a  
342 complement to the regional assessments carried out by tuna RFMOs. We assess the “local  
343 tuna stocks” in the EEZ of Côte d'Ivoire by estimating abundance indices. The abundance  
344 indices obtained by using VAST served as inputs to other methods to characterize their  
345 seasonal and inter-annual variability. In this study, for the sake of simplicity, we used the term  
346 “local tuna stock” somewhat inappropriately, because tuna are migratory so the stock concept  
347 is more complex than a spatial boundary. We agree with Amon Kothias and Bard (1993)  
348 when they define the tuna resources of Côte d'Ivoire as a component of the tropical Atlantic  
349 tuna stocks. The estimated abundance indices are therefore interpreted as the tuna outflow  
350 remaining in the study area at a given time. In addition, the study area is imperfectly assigned  
351 to the Ivorian EEZ, but the selected area extends beyond the Ivorian EEZ and considers  
352 boundary effects. One of the major limitations of this study is the selection of the fishery.  
353 Several fleets and gear types exploit the tuna resources of the Ivorian EEZ, but our study was  
354 limited to the French and Spanish purse seiners. This choice enhances consistency due to the  
355 relatively better quality and availability of the data, but interpretations may be affected by  
356 gear selectivity. It is important to consider these factors in the conclusions of this research, but  
357 as far as we know, this study is the first to estimate a local abundance of tunas with such  
358 levels of disaggregation (maturity level and school type) in the Gulf of Guinea region.

359 Another major limitation of this study is the use of commercial catch and effort  
360 information to estimate abundance indices. The relationship between standardized CPUEs and

361 real abundance can be subject to hyperdepletion or hyperstability, depending on the fishing  
362 gear (Hilborn and Walters, 1992; Walters, 2003). Tropical purse seine tuna fisheries rely on  
363 many factors such as the concentration of schools in clusters (Fonteneau et al., 2017, 2008;  
364 Orensanz et al., 1998), and on the continuous introduction of technological developments  
365 (e.g., FADs equipped with echosounders) that contribute to the increase in vessels' fishing  
366 power (Fonteneau et al., 1999; Torres-Irineo et al., 2014). However, due to the difficulties in  
367 obtaining information on new fishing technology introduced on board each vessel, the  
368 conventional standardization methods do not really capture the impact of these factors. We  
369 know that the estimated abundance indices in this paper are not immune to the biases from  
370 which the approximation of abundance by standardized CPUE suffers. However, we have  
371 chosen to disaggregate the data by school type and maturity stage to avoid some biases.

372 With regards to the effects of the environmental conditions on tuna resources, studies have  
373 shown that in comparison with other tuna species, skipjack tuna vertical movements are  
374 limited and restricted to surface waters because they have a limited tolerance to low levels of  
375 dissolved oxygen and very low temperatures (Graham and Dickson, 2004). The fact that the  
376 dissolved oxygen at a depth of 100 meters, MLD and SST better explain the variability in  
377 skipjack catch rate is due in part to this species-specific characteristic. Our results showed that  
378 the peak season of skipjack tuna in Côte d'Ivoire (August – December) coincides with the  
379 presence of upwelling, rich in nutrients, during the third quarter of the year. Skipjack tuna are  
380 most concentrated inside the EEZ of Côte d'Ivoire during the months with low SST and high  
381 CHL (i.e. from August to December with a peak in September) (supplementary material S1:  
382 Fig. 2:S1 and Fig. 9:S1). Bard et al. (1988) suggested that the equatorial migration of skipjack  
383 tuna is particularly driven by foraging and thus driven by particularly productive zones. The  
384 delay of 1-2 months from the peak of the upwelling to the peak of skipjack abundance  
385 provides further evidence confirming these general aspects already analysed in the Gulf of  
386 Guinea. Indeed, Mendelsohn and Roy (1986) found that higher concentrations of skipjack  
387 occur when there was an upwelling one month prior to fishing, followed by a relative  
388 warming of the waters two weeks prior to fishing. Our results reinforce this observation while  
389 highlighting the differences observed between dFADs and FSC fishing. Mature yellowfin  
390 tuna are most concentrated inside the EEZ of Côte d'Ivoire during the months with high SST  
391 and high SSH (i.e., from March to July with a peak in April - May) (supplementary material:  
392 Fig. 2: S1 and Fig. 9:S1). Several studies have shown that there is significant yellowfin  
393 spawning activity in the Gulf of Guinea from December through April (ICCAT, 2019). The  
394 seasonality of adult yellowfin tuna in this study is consistent with previous findings in this  
395 sub-area of the Gulf of Guinea. The peak in abundance is due to a mixture of genetic  
396 migrations related to reproduction which takes place in the first quarter of the year in the  
397 study area (Albaret, 1977) and trophic migrations related to the enrichment of the study area  
398 in food generated by the presence of coastal upwelling which takes place from January to  
399 February (Binet, 1976). In conclusion, the seasonality of tuna abundance in the EEZ of Côte  
400 d'Ivoire is consistent with the patterns of tropical tuna characteristics observed at regional  
401 scales and a function of local environmental conditions (Mendelsohn and Roy, 1986).

402 The recent stock assessments of Atlantic tropical tunas have revealed that (1) yellowfin  
403 tuna is not overfished and not subject to overfishing, (2) bigeye tuna has been overfished  
404 since 1994 and overfishing has been undergoing since 1997, and (3) skipjack tuna are not  
405 likely overfished and not subject to overfishing (ICCAT, 2019). When stocks are overfished,  
406 one can expect a reduction in biomass, the impact of which is greater at the periphery of the  
407 spatial distribution of the stock (e.g., in the EEZ of Côte d'Ivoire) than in the core area, as  
408 postulated by the McCall's basin hypothesis (MacCall, 1990). For bigeye, the tropical tuna  
409 species most impacted by exploitation, our results suggest a declining trend during the first  
410 decade and an increasing trend from 2009 onwards on dFADs and 2014 on FSC components.

411 The overall trend of bigeye caught on FSC varies slightly from 2000 to 2017 followed by a  
412 sudden increase in the last two years (Fig. 3 S1). It is very unlikely to see such an abrupt  
413 change in the abundance of a long-lived species such as bigeye. The resulting overall trend  
414 could be due to a change in catchability compared to previous years. We reserve the right to  
415 interpret it as a change in the abundance of this species. However, since bigeye is rare in this  
416 area, a peak in moderate catches could generate such observations. The situation is somewhat  
417 different for catches on dFADs. More specific analyses could help better understand the  
418 phenomenon observed in the abundance indices of mature bigeye tuna in this study area. The  
419 situation is different for yellowfin and skipjack as both species show a general downward  
420 trend, with the exception of yellowfin captured on FSC. As we have seen, CHL and SST are  
421 responsible for seasonality in abundance indices of skipjack and mature yellowfin. The global  
422 trend of these variables over the study period could have affected the overall dynamics of the  
423 abundance of both species. Indeed, there is an overall upward trend in SST, and a downward  
424 trend in the coastal upwelling index and chlorophyll concentration over the years (Fig. 9).  
425 Future analyses more specific to this topic will explain the similarity between trends in these  
426 variables and those of some abundance indices estimated in this paper.

427 Several studies have examined the difference between the behaviour of tropical tuna  
428 captured on dFADs or on FSC, and differences in several biological parameters and migrating  
429 patterns have been reported (Hallier and Gaertner, 2008). Ménard et al. (2000) suggested that  
430 the dFADs fishery may have wide-ranging effects on the migration of tuna in general and on  
431 the productivity of skipjack in particular. Coming back to the results of the univariate analysis  
432 of the relationship of tuna abundance with environmental variables (Table 5, Table 5), the  
433 importance of the dissolved oxygen at 100 meter depth (DO2\_100) on the abundance of  
434 skipjack can be seen by the percentage of the variance explained: 35.7% on FSC against only  
435 23.3% on dFADs.

436 In addition, CHL explains 9.58% of the catches on FSC but very little (0.14%) on dFADs.  
437 Consequently, as skipjack caught on dFADs are comparable in size with individuals caught  
438 on FSC, this suggests that dFADs decrease the dependence of skipjack on several  
439 environmental factors that is to say modify its habitat. Moreover, the peak abundance of  
440 skipjack catches on dFADs take place one to two months before the peak abundance of  
441 catches on free school in a period which could be less favourable in terms of habitat. Some  
442 differences in deviance explained (by environmental variables) were also observed between  
443 catches on dFADs and catches on FSC for the other categories studied.

444 Our results suggest that, at the same level of maturity for the same species, the effect of  
445 environmental variables on abundance indices differ between dFADs and FSC. These  
446 differing effects of environmental variables on tuna abundance have been observed in several  
447 studies (Druon et al., 2017; Zainuddin et al., 2019) without reaching a definitive conclusion  
448 on how large is the effect of dFAD use on tuna populations.

## 449 **5. Conclusion**

450 This study highlighted the details of local resources of regionally managed highly migratory  
451 species like tropical tunas. General trend and seasonality of such local resources has been  
452 assessed and analysed. In an international context where competitiveness is at stake, such  
453 analyses with complementary characteristics are essential to better take advantage of the share  
454 of global resources over which a country has some rights. This study constitutes one of the  
455 proofs of the possibility for some coastal countries to evaluate the variations in abundance of  
456 tunas in the waters under their jurisdiction in addition to the broad-scale patterns which are  
457 analysed within RFMOs. It revealed changes in abundance indices over the study period (Fig.  
458 7); reductions in amplitude of the seasonality for some combination of species-size categories  
459 (Fig. 5) and differences in peak abundance and sensitivity to environmental variability

460 between dFADs and free school fishing (Tables 4 and 5). For skipjack, our results indicate  
461 that dFAD-associated schools are less dependent on the variation of several environmental  
462 factors than free schools. Our results suggest a strong relationship between the dynamics of  
463 some environmental variables and the abundance indices for skipjack and adult yellowfin  
464 tunas. This study made it possible to isolate the particularities of the local resource and thus to  
465 lay the first bases for possible analyses of the influence of global phenomena (overfishing,  
466 climate change, etc.) on the local resource at the EEZ level, thus providing the basis for future  
467 management measures.  
468

469 **Declaration of competing interest**

470 The authors declare that they have no known competing financial interests or personal  
471 relationships that could have appeared to influence the work reported in this paper.

472

473 **Credit authorship contribution statement**

474 **S. AKIA**: Conceptualization, Methodology, Software, Validation, Visualization,  
475 Investigation, Writing - original draft.

476 **M. Amande**: Conceptualization, Supervision, Writing - review & editing, Supervision.

477 **D. Gaertner**: Conceptualization, Resources, Validation, Writing - review & editing,  
478 Supervision, Funding acquisition, Project administration.

479 **P. Pascual**: Data Curation, Writing - review & editing.

480

481 **Acknowledgements**

482 This project was co-funded by IRD (ARTS funding) and the “Observatoire des Ecosystèmes  
483 Pélagiques Tropicaux exploités” (Ob7) from IRD/MARBEC. We sincerely thank the  
484 contribution of the staff of the Ob7 for providing data on the French fleet. The authors also  
485 thank Lorelei Guery, Francis Marsac and Hervé Demarq (IRD-MARBEC) for many helpful  
486 suggestions, advices and methodological tools regarding our analyses.

487 Our gratitude also goes to the reviewers of this manuscript for their comments, corrections  
488 and suggestions for its improvement.

489

490

491

492

493

494

495

496

497

498

499

500

501

502 **Tables and figures**

503

504 **Tables**

505

506 Table 1 :

507 Summary of the candidate environmental variables included in this study

<b>Variable acronym</b>	<b>Variable name</b>	<b>Unit</b>
SST	Sea surface temperature	°C
SSH	Sea surface height	meter
CHL	Chlorophyll concentration	mg. m <sup>-3</sup>
DO2_100	Dissolved oxygen concentration at 100 meters of depth	mmol.m <sup>-3</sup>
SSS	Salinity	PSU
MLD	Mixed layer thickness	meter
CUI_sst	Coastal upwelling index	°C

508

509

510

511 Table 2 :

512 Summary of the seasonal variability of abundance indices in the EEZ of Côte d'Ivoire (2000-  
513 2019).

<b>Period</b>	<b>Seasonal factor (Peak-lowest)</b>	<b>Peak month</b>	<b>Peak abundance season</b>	<b>Low abundance season</b>	<b>Change in seasonality over the study period</b>
Mat_BET_FdADs	21.03	August	June-October	Novemb-May	Slight shrinkage
Mat_BET_FSC	7.73	June	April-October	Novemb-March	Almost constant
SKJ_FAD	492.3	October	August-Decem	January-July	Almost constant
SKJ_FSC	11.97	December/ April	October-Decem/ March-May	May-September	Shrinkage
Imm_YFT_dFADs	42.9	October	July-December	January-June	Almost constant
Imm_YFT_FSC	8.95	November	August-Septem	January-July	Almost constant
Mat_YFT_dFADs	90.2	August	June-September	November-April	Almost constant
Mat_YFT_FSC	177.13	April	March-July	October-January	Almost constant

514

515

516

517 Table 3:

518 Correlation between variables and dimensions (Dim1), square cosine (cos), contribution  
 519 (contrib) and eigenvalue (inertia) of the first three principal components from the PCA  
 520 analysis for the environmental variables selected in the study.

Variable	Dim.1	contrib	Cos2	Dim.2	contrib	Cos2	Dim.3	contrib	Cos2
SST	-0.90	21.62	0.811	-0.059	0.309	0.004	-0.095	1.044	0.009
SSS	0.654	11.40	0.428	0.431	16.34	0.186	0.386	17.36	0.149
MLD	0.195	1.015	0.038	0.907	72.40	0.823	-0.223	5.815	0.05
CHL	0.914	22.27	0.835	-0.171	2.56	0.029	0.093	1.018	0.009
CUI_sst	0.820	17.95	0.673	-0.280	6.918	0.079	0.073	0.623	0.005
DO2_100	-0.516	7.093	0.266	0.08	0.561	0.006	0.797	74	0.635
SSH	-0.836	18.646	0.7	0.102	0.909	0.01	0.034	0.135	0.001
% Inertia		53.58			16.24			12.62	

521

522

523

524

525 Table 4 :

526 Generalized additive models (univariate) of the eight categories of tuna as functions of seven  
 527 environmental variables. Deviance explained (in percentage) of log (abundance indices) by  
 528 each variable are shown. The symbol \* means that the coefficient is significant at 5% (p-value  
 529 <0.05)

Variable	SKJ_FAD	SKJ_FS	YFT_Mat FAD	YFT_Mat FSC	YFT_Imm FAD	YFT_Imm FSC	BET_Mat FAD	BET_Mat FSC
SST	1.60	12.8*	25.5*	25.7*	1.87	2.14*	37.7*	18.1*
DO2_100	25.1*	32.7*	7.72*	3.94e-05	30.6*	19.8*	17.7*	3.13*
SSH	1.28	5.29*	31.9*	1.85*	3.23*	4.99*	20*	10*
CHL	0.32	12*	24.6*	1.46	0.84	4.05*	31.8*	8.6*
SSS	0.81	13.2*	8.91*	4.46*	0.01	3.87*	17*	11.3*
MLD	2.92*	11*	4.61*	4.26*	0.65	0.72	4.32*	18.1*
CUI_sst	0.14	9.58*	15*	2.24*	7.29e-06	0.63	16*	7.22*

530

531

532

533

534

535 Table 5:

536 Summary of the relationships between environmental variables and abundance indices.  
537 Only factors with explained deviance higher than 10% have been selected and ranked by  
538 decreasing order of explained deviance (e.g. Mature BET on FSC, SST > MLD > SSS >  
539 SSH).

<b>Species</b>	<b>Fishing on dFADs</b>	<b>Fishing on FSC</b>
SKJ	DO2_100	DO2_100 ; SSS ; SST ; CHL ; MLD
Mature YFT	SSH ; SST ; CHL and CUI_sst	SST
Immature YFT	DO2_100	DO2_100
Mature BET	SST ; CHL ; SSH ; DO2_100 ; SSS ; CUI_sst	SST ; MLD ; SSS and SSH

540

541

542

543

544

545

546

547

548

549

550

551

552

553

554

555

556

557

558

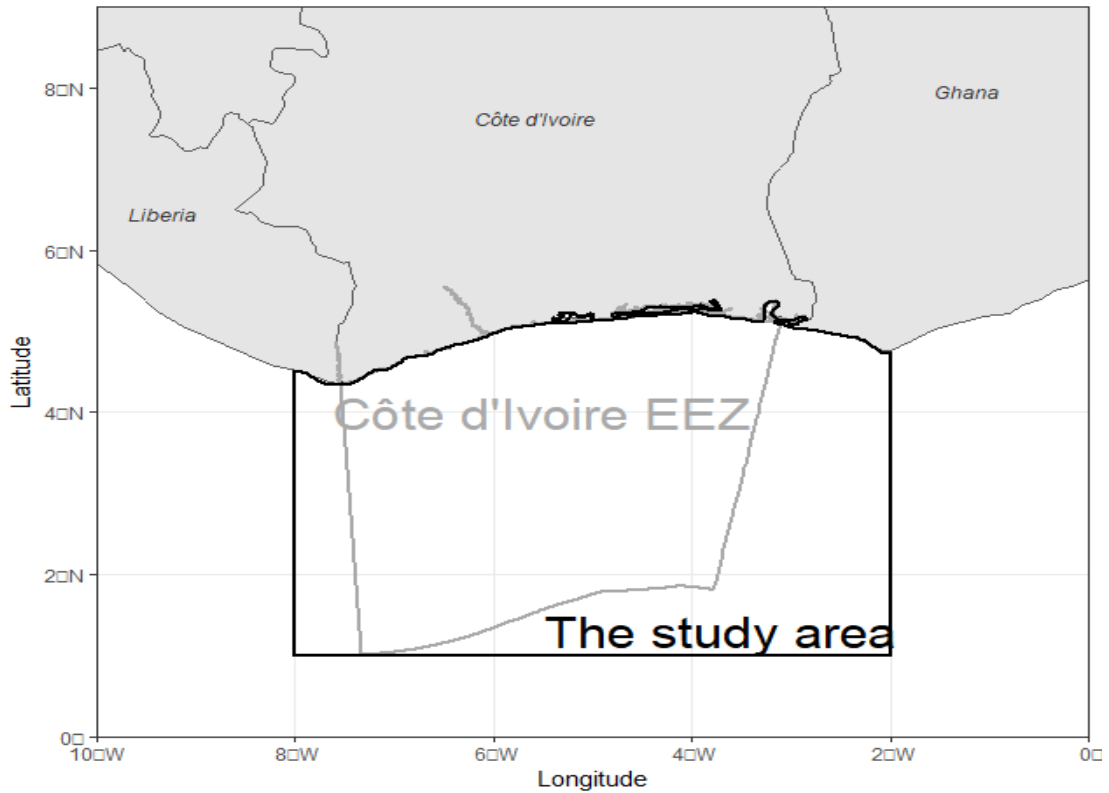
559

560



561

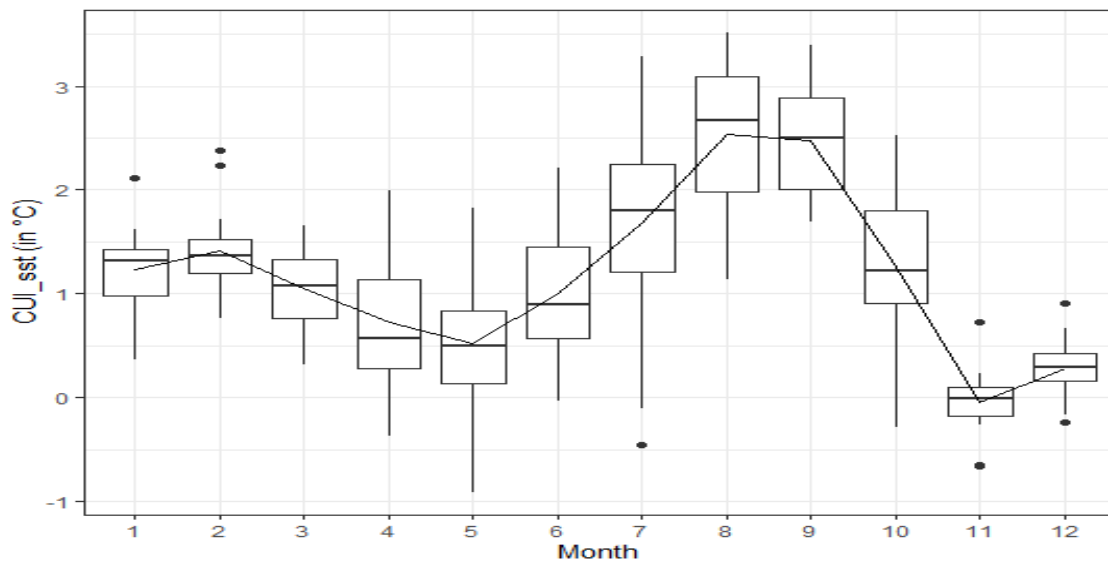
562 **Figures**



563

564 Fig. 1. The EEZ of Côte d'Ivoire and the study area. The area of interest is the square area  
565 defined in this figure.

566



567

568 Fig. 2. Seasonal variations in the SST-based coastal upwelling index in the Ivorian EEZ

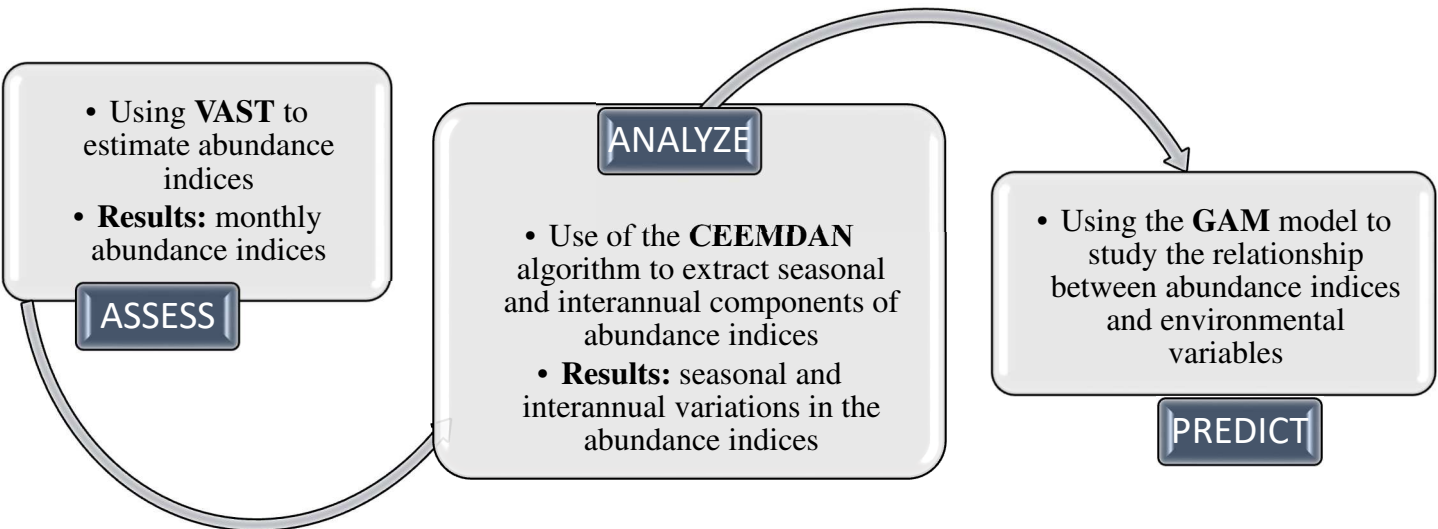
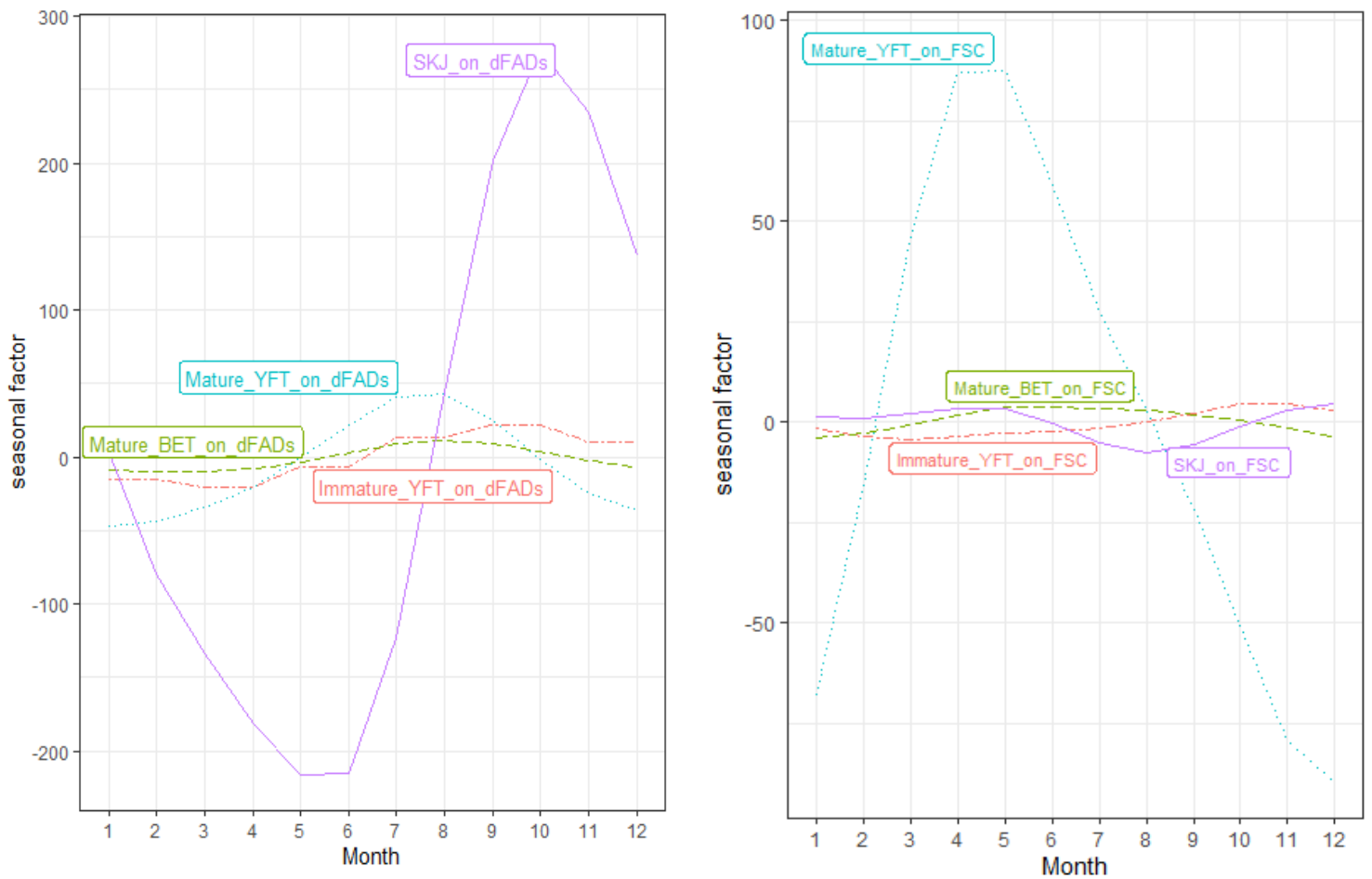
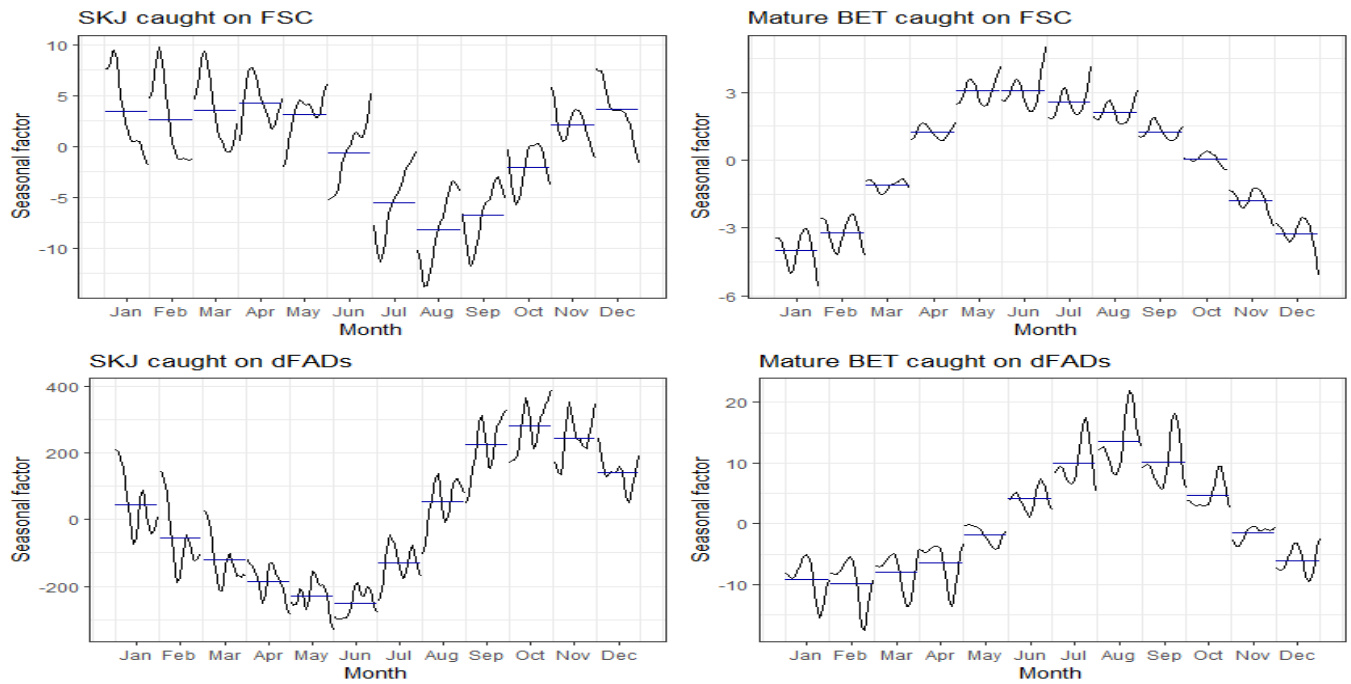


Fig. 1. Schematic representation of the methodology used in this study

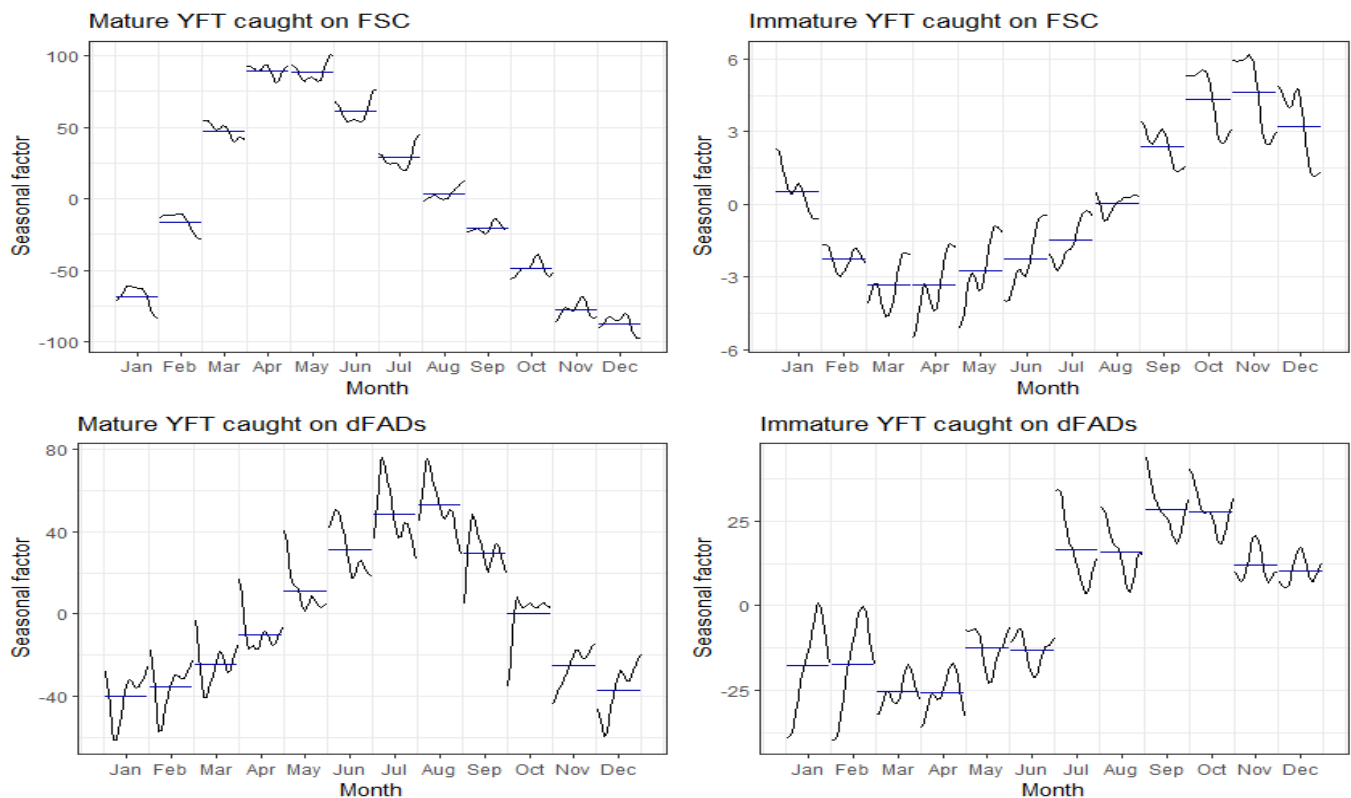


570 Fig. 4. Average monthly changes in abundance indices for eight categories of tropical tuna  
 571 analyzed for the 2000-2019 period.



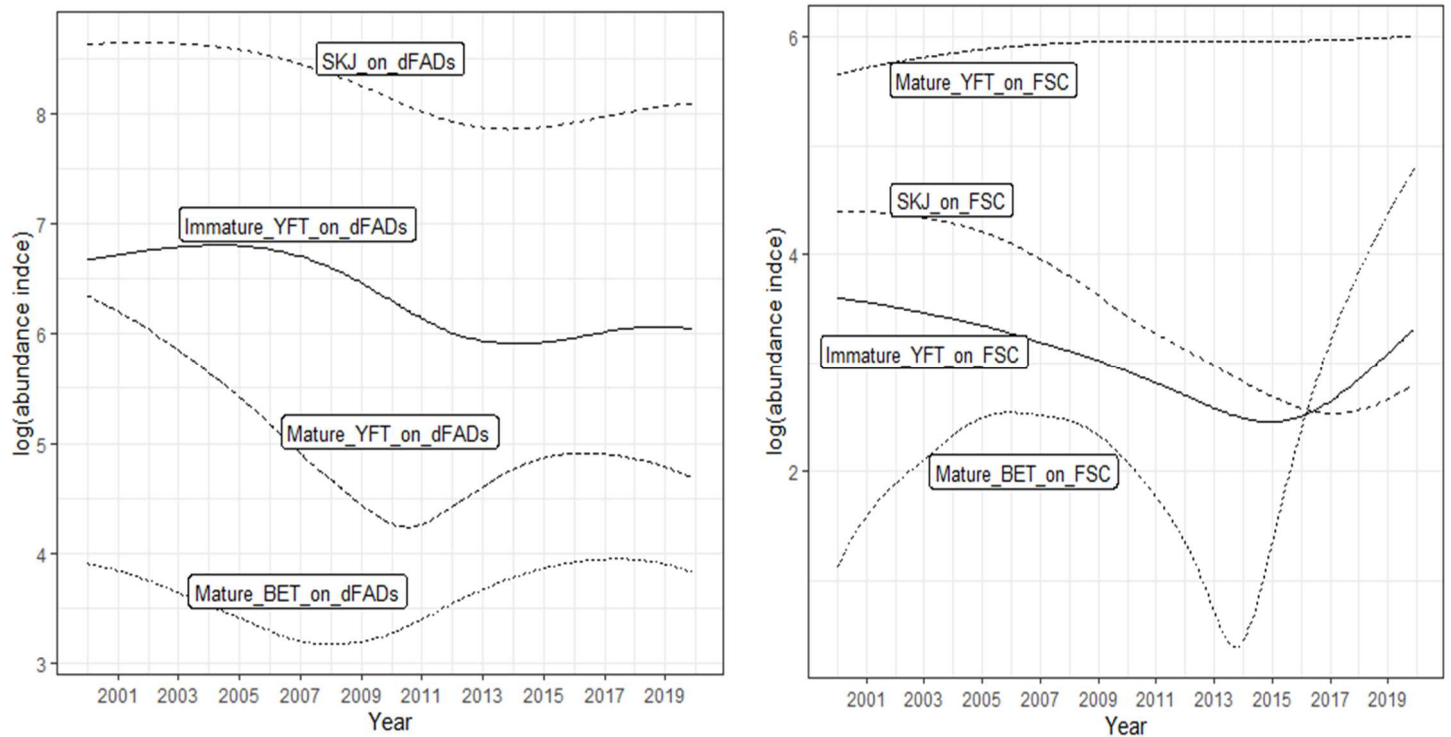
572

573 **Fig. 5.** Interannual variations in monthly abundance indices of skipjack and mature bigeye  
 574 tuna. The curves observed for each month correspond to the interannual variability of  
 575 abundance over that month and the horizontal dashes correspond to the monthly average (in  
 576 trend) over the study period.  
 577

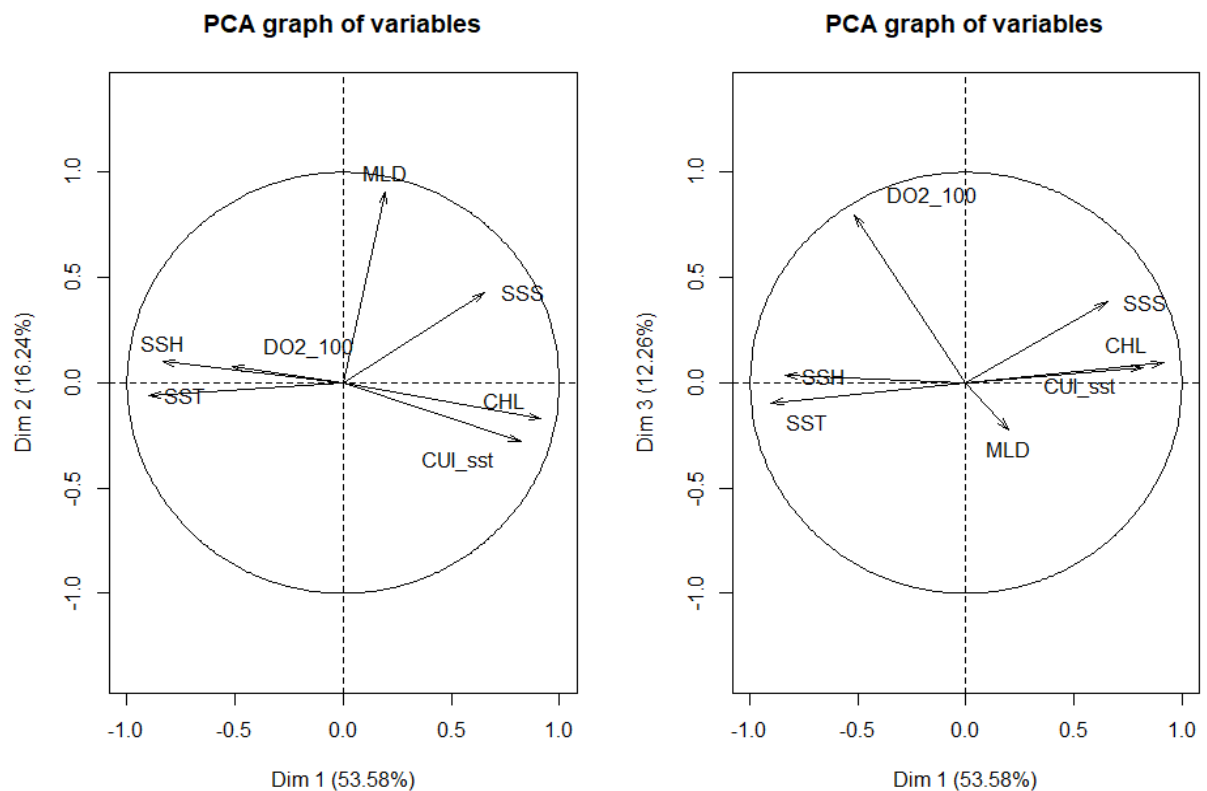


578

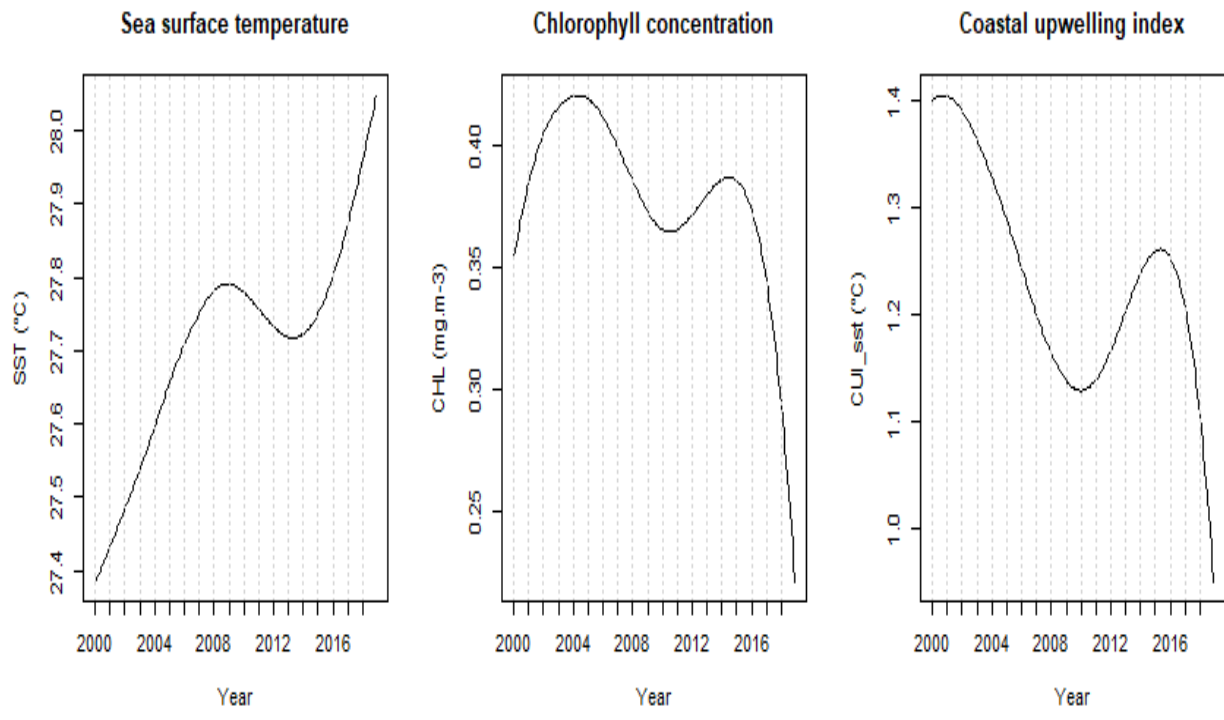
579 **Fig. 6.** Interannual variations in monthly abundance indices of yellowfin tuna. The curves  
 580 observed for each month correspond to the interannual variability of abundance over that  
 581 month and the horizontal dashes correspond to the monthly average (in trend) over the study  
 582 period.



583 Fig. 7. Interannual variations of abundance indices by fishing mode over the period 2000-  
 584 2019.



585  
 586 Fig. 8. First (Dim 1), second (Dim 2) and third (Dim 3) axes of the principal component  
 587 analysis of the sea surface temperature (SST), sea surface height (SSH), sea surface salinity  
 588 (SSS), chlorophyll concentration (CHL), dissolved oxygen at a depth of 100 meters  
 589 (DO2\_100), mixed-layer thickness (MLD) and coastal upwelling index (CUI\_sst) in the EEZ  
 590 of Côte d'Ivoire.



591

592 Fig. 9. Interannual variations (global trend) of three environmental variables over the period  
 593 2000-2018. The decomposition has been done using the CEEMDAN's algorithm.

594

595

596

597

598

599

600

601

602

603

604

605

606

607

608

609

610

611 **References**

- 612 Albaret, J.-J., 1977. La reproduction de l'albacore (*Thunnus albacares*) dans le golfe de Guinée.  
613 O.R.S.T.O..M. série Oceanogr. <https://www.documentation.ird.fr/hor/fdi:19756>
- 614 Albeare, S.M., 2009. Comparisons of Boosted Regression Tree, GLM And GAM Performance In The  
615 Standardization Of Yellowfin Tuna Catch-Rate Data From The Gulf Of Mexico Lonline Fishery.  
616 Thesis. [https://digitalcommons.lsu.edu/gradschool\\_theses/2880](https://digitalcommons.lsu.edu/gradschool_theses/2880)
- 617 Amon Kothias, J., Bard, F., 1993. Les ressources thonières de Côte d'Ivoire 323–352.  
618 <https://www.documentation.ird.fr/hor/fdi:37718>
- 619 Andriamahefazafy, M., 2020. The politics of sustaining tuna, fisheries and livelihoods in the Western  
620 Indian Ocean. <https://www.documentation.ird.fr/hor/fdi:37718>
- 621 Bard, F.-X., Cayré, P., Diouf, T., 1988. Les migrations, in: Ressources, Pêche et Biologie Des Thonidés  
622 Tropicaux de l'Atlantique Centre-Est, Document Technique Sur Les Pêches - FAO. FAO, Rome,  
623 pp. 111–156. <https://www.documentation.ird.fr/hor/fdi:34186>
- 624 Benazzouz, A., Mordane, S., Orbi, A., Chagdali, M., Hilmi, K., Atillah, A., Lluís Pelegrí, J., Hervé, D.,  
625 2014. An improved coastal upwelling index from sea surface temperature using satellite-based  
626 approach - The case of the Canary Current upwelling system. *Cont. Shelf Res.*  
627 <https://doi.org/10.1016/j.csr.2014.03.012>
- 628 Binet, D., 1976. Contribution à l'écologie de quelques taxons du zooplancton de Côte d'Ivoire. 2-  
629 Doliolles, Salpes, Appendiculaires. *Doc. Sci. Cent. Rech. Océanographiques, Abidjan 7*, 45–61.  
630 <https://www.documentation.ird.fr/hor/fdi:32209>
- 631 Campbell, R.A., 2004. CPUE standardisation and the construction of indices of stock abundance in a  
632 spatially varying fishery using general linear models. *Fish. Res.*  
633 <https://doi.org/10.1016/j.fishres.2004.08.026>
- 634 Cofrepeche, Poseidon, M.& N., 2012. Évaluation ex-post du protocole de l'accord de partenariat dans  
635 le domaine de la pêche entre l'Union européenne et la Côte d'Ivoire (Contrat cadre  
636 MARE/2011/01-Lot 3, contrat spécifique 2). [https://op.europa.eu/en/publication-detail/-](https://op.europa.eu/en/publication-detail/-/publication/b2a08ce7-bac1-11e7-a7f8-01aa75ed71a1)  
637 [/publication/b2a08ce7-bac1-11e7-a7f8-01aa75ed71a1](https://op.europa.eu/en/publication-detail/-/publication/b2a08ce7-bac1-11e7-a7f8-01aa75ed71a1)
- 638 Cury, P., Roy, C., 1987. Upwelling et pêche des espèces pélagiques côtières de Côte-d'Ivoire: une  
639 approche globale. *Oceanol. acta 10*, 347–357. <https://archimer.ifremer.fr/doc/00108/21909>
- 640 Druon, J.-N., Chassot, E., Murua, H., Lopez, J., 2017. Skipjack tuna availability for purse seine fisheries  
641 is driven by suitable feeding habitat dynamics in the Atlantic and Indian Oceans. *Front. Mar. Sci.*  
642 *4*, 315. <https://doi.org/10.3389/fmars.2017.00315>
- 643 Duparc, A., Depetris, M., Floch, L., Cauquil, P., Bach, P., Lebranchu, J., 2020. ( T3 ) SOFTWARE A  
644 redesign for the T3 code 22, 1–5. <https://doi.org/10.5281/zenodo.3878125.Changes>
- 645 Failler, P., El Ayoubi, H., Konan, A., 2014. Industrie des pêches et de l'aquaculture en Côte d'Ivoire.  
646 <https://dx.doi.org/10.13140/RG.2.1.2919.1843>
- 647 Fonteneau, A., Alayón, P.J.P., Marsac, F., 2017. Exploitation of large yellowfin tuna caught in free  
648 schools concentrations during the 2013 spawning season (December 2012-May 2013). *Collect.*  
649 *Vol. Sci. Pap. ICCAT 73*, 868–882. <https://www.documentation.ird.fr/hor/fdi:010072540>
- 650 Fonteneau, A., Gaertner, D., Nordstrom, V., 1999. An overview of problems in the CPUE-abundance  
651 relationship for the tropical purse seine fisheries. *Collect. Vol. Sci. Pap. ICCAT 49*, 259–276.  
652 <https://www.documentation.ird.fr/hor/fdi:010045940>

653 Fonteneau, A., Lucas, V., Tewkai, E., Delgado, A., Demarcq, H., 2008. Mesoscale exploitation of a  
654 major tuna concentration in the Indian Ocean. *Aquat. Living Resour.* 21, 109–121.  
655 <https://doi.org/10.1051/alr:2008028>

656 Graham, J.B., Dickson, K.A., 2004. Tuna comparative physiology. *J. Exp. Biol.*  
657 <https://doi.org/10.1242/jeb.01267>

658 Hallier, J.P., Gaertner, D., 2008. Drifting fish aggregation devices could act as an ecological trap for  
659 tropical tuna species. *Mar. Ecol. Prog. Ser.* <https://doi.org/10.3354/meps07180>

660 Hastie, T., Tibshirani, R., 1987. Generalized additive models: Some applications. *J. Am. Stat. Assoc.*  
661 <https://doi.org/10.1080/01621459.1987.10478440>

662 Hilborn, R., Walters, C.J., 1992. Stock and recruitment, in: *Quantitative Fisheries Stock Assessment.*  
663 Springer, pp. 241–296. [https://link.springer.com/chapter/10.1007/978-1-4615-3598-0\\_7](https://link.springer.com/chapter/10.1007/978-1-4615-3598-0_7)

664 Huang, N., Shen, Z., Long, S., Wu, M., Shih ..., H., 1998. The empirical mode decomposition and the  
665 Hilbert spectrum for nonlinear and non-stationary. *Proc. Math.*  
666 <https://doi.org/10.1098/rspa.1998.0193>

667 Husson, F., 2008. FactoMineR: An R Package for Multivariate Analysis.  
668 <https://doi.org/10.18637/jss.v025.i01>

669 Hyndman, R.J., Khandakar, Y., 2008. Automatic time series forecasting: the forecast package for R. *J.*  
670 *Stat. Softw.* 27, 1–22. <https://doi.org/10.18637/jss.v027.i03>

671 ICCAT, 2019. Report for Biennial Period, 2018-2019, Part II – Vol. 2. Standing Committee on Research  
672 and Statistics (SCRS). Madrid, Spain 470. [https://iccat.int/en/pubs\\_biennial.html](https://iccat.int/en/pubs_biennial.html)

673 Kaiser, H.F., 1960. The application of electronic computers to factor analysis. *Educational and*  
674 *Psychological Measurement.* *Educ. Psychol. Meas.*  
675 <https://doi.org/10.1177/001316446002000116>

676 Katara, I., Gaertner, D., Marsac, F., Grande, M., Kaplan, D., Agurtzane, U., Lorelei, G., Mathieu, D.,  
677 Antoine, D., Laurent, F., Jon, L., Francisco, A., 2018. Standardisation of yellowfin tuna CPUE for  
678 the EU purse seine fleet operating in the Indian Ocean., 19th Working Party on Tropical Tunas.  
679 <https://www.iotc.org/documents/WPTT/20/36>

680 Lehodey, P., Alheit, J., Barange, M., Baumgartner, T., Beaugrand, G., Drinkwater, K., Fromentin, J.M.,  
681 Hare, S.R., Ottersen, G., Perry, R.I., Roy, C., van der Lingen, C.D., Werner, F., 2006. Climate  
682 variability, fish, and fisheries. *J. Clim.* <https://doi.org/10.1175/JCLI3898.1>

683 Luukko, P.J.J., Helske, J., Räsänen, E., 2016. Introducing libeemd: a program package for performing  
684 the ensemble empirical mode decomposition. *Comput. Stat.* [https://doi.org/10.1007/s00180-](https://doi.org/10.1007/s00180-015-0603-9)  
685 [015-0603-9](https://doi.org/10.1007/s00180-015-0603-9)

686 MacCall, A.D., 1990. Dynamic geography of marine fish populations. Washington Sea Grant Program  
687 Seattle, WA. <https://doi.org/10.1086/417298>

688 Marsac, F., 2017. The Seychelles Tuna Fishery and Climate Change, in: *Climate Change Impacts on*  
689 *Fisheries and Aquaculture.* <https://doi.org/10.1002/9781119154051.ch16>

690 Maunder, M.N., Langley, A.D., 2004. Integrating the standardization of catch-per-unit-of-effort into  
691 stock assessment models: testing a population dynamics model and using multiple data types.  
692 *Fish. Res.* 70, 389–395. <https://doi.org/10.1016/j.fishres.2004.08.015>

693 Maunder, M.N., Punt, A.E., 2004. Standardizing catch and effort data: A review of recent approaches.  
694 *Fish. Res.* <https://doi.org/10.1016/j.fishres.2004.08.002>

695 Maunder, M.N., Thorson, J.T., Xu, H., Oliveros-Ramos, R., Hoyle, S.D., Tremblay-Boyer, L., Lee, H.H.,  
696 Kai, M., Chang, S.K., Kitakado, T., Albertsen, C.M., Minte-Vera, C. V., Lennert-Cody, C.E., Aires-  
697 da-Silva, A.M., Piner, K.R., 2020. The need for spatio-temporal modeling to determine catch-  
698 per-unit effort based indices of abundance and associated composition data for inclusion in  
699 stock assessment models. *Fish. Res.* 229, 105594.  
700 <https://doi.org/10.1016/j.fishres.2020.105594>

701 Maury, O., Gascuel, D., Marsac, F., Fonteneau, A., Rosa, A.-L. De, 2001. Hierarchical interpretation of  
702 nonlinear relationships linking yellowfin tuna (*Thunnus albacares*) distribution to the  
703 environment in the Atlantic Ocean. *Can. J. Fish. Aquat. Sci.* [https://doi.org/10.1139/cjfas-58-3-](https://doi.org/10.1139/cjfas-58-3-458)  
704 458

705 Ménard, F., Fonteneau, A., Gaertner, D., Nordstrom, V., Stéquert, B., Marchal, E., 2000. Exploitation  
706 of small tunas by a purse-seine fishery with fish aggregating devices and their feeding ecology in  
707 an eastern tropical Atlantic ecosystem, in: *ICES Journal of Marine Science*.  
708 <https://doi.org/10.1006/jmsc.2000.0717>

709 Ménard, F., Marsac, F., Bellier, E., Cazelles, B., 2007. Climatic oscillations and tuna catch rates in the  
710 Indian Ocean: A wavelet approach to time series analysis. *Fish. Oceanogr.*  
711 <https://doi.org/10.1111/j.1365-2419.2006.00415.x>

712 Mendelssohn, R., Roy, C., 1986. Environmental influences on the French, Ivory-Coast, Senegalese and  
713 Moroccan tuna catches in the Gulf of Guinea, in: *Proceedings of the ICCAT Conference on the*  
714 *International Skipjack Year Program*. Edited by EK Symons, PM Miyake, and GT Sakagawa.  
715 ICCAT, Madrid. pp. 170–188. <https://www.documentation.ird.fr/hor/fdi:23990>

716 Monin, J.A., Amalatchy, J.N.C., Goran, D.K.N., Chris, M.N.C., Kouadio, F.K., Kouadio, C., Nadège, A.,  
717 Dewals, P., Restrepo, V., 2017. UTILIZATION AND TRADE OF FAUX POISSON LANDED IN ABIDJAN  
718 73, 749–754. <https://www.documentation.ird.fr/hor/fdi:010072530>

719 Moreno, G., Dagorn, L., Sancho, G., Itano, D., 2007. Fish behaviour from fishers' knowledge : the case  
720 study of tropical tuna around drifting fish aggregating devices ( DFADs ) 1528, 1517–1528.  
721 <https://doi.org/10.1139/F07-113>

722 Morlière, A., 1970. Les saisons marines devant Abidjan. *Doc. Sci. Cent. Rech. Océanographiques,*  
723 *Abidjan* 1, 1–15. <http://aquaticcommons.org/id/eprint/7953>

724 Orensanz, J.M., Parma, A.M., Hall, M.A., 1998. The analysis of concentration and crowding in shellfish  
725 research. *Can. Spec. Publ. Fish. Aquat. Sci.* 143–158.  
726 <https://www.researchgate.net/publication/268215919>

727 Pallarés, P., Hallier, J.P., 1997. Analyse du schéma d'échantillonnage multispécifique des thonidés  
728 tropicaux. *Rapp. Sci. IEO/ORSTOM, Program.* 95, 37.

729 Putri, A.R.S., Zainuddin, M., Musbir, M., Mustapha, M.A., Hidayat, R., 2019. Effect of oceanographic  
730 conditions on skipjack tuna catches from FAD versus free-swimming school fishing in the  
731 Makassar Strait, in: *IOP Conference Series: Earth and Environmental Science*. p. 12008.  
732 <https://doi.org/10.1088/1755-1315/370/1/012008>

733 R Core Team, 2019. R: A language and environment for statistical computing. *R Found. Stat. Comput.*  
734 <https://www.R-project.org>

735 Ricker, W.E., 1940. Relation of "Catch per Unit Effort" to Abundance and Rate of Exploitation. *J. Fish.*  
736 *Res. Board Canada.* <https://doi.org/10.1139/f40-008>

737 Romagny, B., Ménard, F., Dewals, P., Gaertner, D., N'Goran, N., 2000. Le "faux-poisson" d'Abidjan et  
738 la pêche sous DCP dérivants dans l'Atlantique tropical Est : circuit de commercialisation et rôle



739 socio-économique. Pêche thonière Dispos. Conc. Poisson. Caribbean-Martinique, 15-19 Oct  
740 1999 634–652. <https://archimer.ifremer.fr/doc/00042/15318>

741 Roudaut, G., 1999. Les relations thons-environnement dans les pêcheries de la zone Sénégal-  
742 Mauritanie: rapport de stage. <https://www.documentation.ird.fr/hor/fdi:010021678>

743 Sax, C., Eddelbuettel, D., 2018. Seasonal Adjustment by {X-13ARIMA-SEATS} in {R}. *J. Stat. Softw.* 87,  
744 1–17. <https://doi.org/10.18637/jss.v087.i11>

745 Thorson, J.T., 2019. Guidance for decisions using the Vector Autoregressive Spatio-Temporal (VAST)  
746 package in stock, ecosystem, habitat and climate assessments. *Fish. Res.*  
747 <https://doi.org/10.1016/j.fishres.2018.10.013>

748 Thorson, J.T., 2018. Three problems with the conventional delta-model for biomass sampling data,  
749 and a computationally efficient alternative. *Can. J. Fish. Aquat. Sci.*  
750 <https://doi.org/10.1139/cjfas-2017-0266>

751 Thorson, J.T., Adams, C.F., Brooks, E.N., Eisner, L.B., Kimmel, D.G., Legault, C.M., Rogers, L.A.,  
752 Yasumiishi, E.M., 2020a. Seasonal and interannual variation in spatio-temporal models for index  
753 standardization and phenology studies. *ICES J. Mar. Sci.*  
754 <https://doi.org/10.1093/icesjms/fsaa074>

755 Thorson, J.T., Maunder, M.N., Punt, E., 2020b. The development of spatio-temporal models of fishery  
756 catch-per-unit-effort data to derive indices of relative abundance. *Fish. Res.*  
757 <https://doi.org/10.1016/j.fishres.2020.105611>

758 Torres-Irineo, E., Gaertner, D., Chassot, E., Dreyfus-León, M., 2014. Changes in fishing power and  
759 fishing strategies driven by new technologies: The case of tropical tuna purse seiners in the  
760 eastern Atlantic Ocean. *Fish. Res.* <https://doi.org/10.1016/j.fishres.2014.02.017>

761 Torres, M.E., Colominas, M.A., Schlotthauer, G., Flandrin, P., 2011. A complete ensemble empirical  
762 mode decomposition with adaptive noise, in: *ICASSP, IEEE International Conference on*  
763 *Acoustics, Speech and Signal Processing - Proceedings.*  
764 <https://doi.org/10.1109/ICASSP.2011.5947265>

765 Walters, C., 2003. Folly and fantasy in the analysis of spatial catch rate data. *Can. J. Fish. Aquat. Sci.*  
766 60, 1433–1436. <https://doi.org/10.1139/f03-152>

767 Wood, S.N., 2017. *Generalized additive models: An introduction with R, second edition, Generalized*  
768 *Additive Models: An Introduction with R, Second Edition.*  
769 <https://doi.org/10.1201/9781315370279>

770 Wu, Z., Huang, N.E., 2009. Ensemble empirical mode decomposition: A noise-assisted data analysis  
771 method. *Adv. Adapt. Data Anal.* <https://doi.org/10.1142/S1793536909000047>

772 Yang, S., Zhang, Y., Zhang, H., Fan, W., 2015. Comparison and analysis of different model algorithms  
773 for CPUE standardization in fishery. *Nongye Gongcheng Xuebao/Transactions Chinese Soc.*  
774 *Agric. Eng.* <https://doi.org/10.11975/j.issn.1002-6819.2015.21.034>

775 Zainuddin, M., Safruddin, Ridwan, M., Putri, A.R.S., Hidayat, R., 2019. The Effect of Oceanographic  
776 Factors on Skipjack Tuna Fad vs Free School Catch in The Bone Bay, Indonesia: An Important  
777 Step Toward Fishing Management. *J. Ilmu Dan Teknol. Kelaut. Trop.* 11, 123–130.  
778 <https://doi.org/10.29244/jitkt.v11i1.24775>

779